Published in final edited form as:
Cancer Prev Res (Phila). 2013 December ; 6(12): . doi:10.1158/1940-6207.CAPR-13-0134.

Isoangustone A, a novel licorice compound, inhibits cell proliferation by targeting PI3-K, MKK4 and MKK7 in human melanoma

Nu Ry Song[1,3,*], **Eunjung Lee**[2,*], **Sanguine Byun**[1,2,3], **Jong-Eun Kim**[1,2], **Madhusoodanan Mottamal**[1], **Jung Han Yoon Park**[4], **Soon Sung Lim**[4], **Ann M. Bode**[1], **Hyong Joo Lee**[2], **Ki Won Lee**[2,3], and **Zigang Dong**[1]

[1]Department of Cellular and Molecular Biology, The Hormel Institute, University of Minnesota, MN 55912, USA

[2]WCU Biomodulation Major, Department of Agricultural Biotechnology and Center for Food and Bioconvergence, Seoul National University, Seoul 151-921, Republic of Korea

[3]Advanced Institutes of Convergence Technology, Seoul National University, Suwon 443-270, Republic of Korea

[4]Department of Food Science and Nutrition, Hallym University, Chuncheon, 200-702, Republic of Korea

Abstract

Licorice root is known to possess various bioactivities, including anti-inflammatory and anticancer effects. Glycyrrhizin (Gc), a triterpene compound, is the most abundant constituent of dried licorice root. However, high intake or long-term consumption of Gc causes several side effects, such as hypertension, hypertensive encephalopathy, and hypokalemia. Therefore, finding additional active compounds other than Gc in licorice that exhibit anticancer effects is worthwhile. We found that isoangustone A (IAA), a novel flavonoid from licorice root, suppressed proliferation of human melanoma cells. IAA significantly blocked cell cycle progression at the G1 phase and inhibited the expression of G1-phase regulatory proteins, including cyclin D1 and cyclin E in the SK-MEL-28 human melanoma cell line. IAA suppressed the phosphorylation of Akt, GSK3β and JNK1/2. IAA also bound to phosphatidylinositol 3-kinase (PI3-K), MKK4, and MKK7, strongly inhibiting their kinase activities in an ATP-competitive manner. Moreover, in a xenograft mouse model, IAA significantly decreased tumor growth, volume, and weight of SK-MEL-28 xenografts. Collectively, these results suggest that PI3-K, MKK4, and MKK7 are the primary molecular targets of IAA in the suppression of cell proliferation. This insight into the biological actions of IAA provides a molecular basis for the potential development of a new chemotherapeutic agent.

Correspondence should be addressed to: Zigang Dong, The Hormel Institute, University of Minnesota, 801 16th Avenue NE, Austin, MN 55912, USA. Tel: 507-437-9600; Fax: 507-437-9606; zgdong@hi.umn.edu or Ki Won Lee, WCU Biomodulation Major, Department of Agricultural Biotechnology, Seoul National University, Seoul 151-742, Republic of Korea. Fax: 82-2-873-5095; kiwon@snu.ac.kr.
*These authors contributed equally to this work.

Cell Authentication: Cells were cytogenetically tested and authenticated before being frozen. The vial of frozen SK-MEL-28 cells was thawed and maintained for 3 months (29 passages). Each vial of frozen SK-MEL-5, SK-MEL-2, and WM-266-4 was thawed and maintained for 2 weeks (5 passages).

The authors declare no conflict of interest.

Keywords

Isoangustone A; PI3K; MKK4; MKK7; melanoma

Introduction

The root of the licorice (*Glycyrrhiza*) plant species has been used in herbal medicine. Multiple lines of evidence have shown that licorice root possesses antioxidant, anti-inflammatory, antiviral, antitumor, hepatoprotective, and cardioprotective bioactivities (1–4). Glycyrrhizin (Gc), a triterpene compound, is considered the principal biologically active component of licorice (4). Therefore, many studies have focused on the bioactivity of Gc. Previous studies demonstrated that licorice and Gc can attenuate inflammation, melanoma cell proliferation, and metastasis both *in vitro* and *in vivo* (5–7). However, long-term consumption of Gc results in undesirable mineralocorticoid excess, hypertension, and hypokalemia. Hypertension is caused by reduction in the activity of 11β-hydroxysteroid dehydrogenase type 2 by glycyrrhetic acid, a metabolite of Gc generated in the intestine (4, 8–9). Therefore, finding additional active anticancer compounds in licorice other than Gc is appropriate.

Uncontrolled proliferation is one of the most critical characteristics of cancer cells (10). Deregulation of cell cycle leads to increased proliferation and carcinogenesis (11). Passage through the cell cycle is strictly controlled by cyclin/cyclin-dependent kinase (CDK) complexes (12). Cyclins D and E bind to CDK4/6 and CDK2, respectively, and sequentially phosphorylate the retinoblastoma protein (Rb). This facilitates the transition from G1 to S phase (13). Amplification of the *cyclin D1* gene and overexpression of the cyclin D1 protein are found in several cancer types, including parathyroid adenoma, breast, colon, lymphoma, prostate, and melanoma (14–16). Cyclin D1 plays a prominent role in driving tumorigenesis (17). Melanoma shows mutations and/or amplification of receptor tyrosine kinases and amplification of the *cyclin D1* and *cdk4* genes, which regulate cell cycle progression (18–19). Thus, inhibition of cyclin D1 expression could be a promising anticancer strategy for melanoma.

Various signaling pathways regulating cell cycle progression have been reported. The mitogen-activated protein kinase (MAPK) signaling pathways play important roles in many biological processes, including cell cycle progression, proliferation, inflammation, apoptosis, and differentiation. The MAPKs include extracellular signal-regulated kinases (ERKs), c-Jun N-terminal kinases (JNKs), and p38. They are activated by specific mitogen-activated protein kinase kinases (MAPKKs), including mitogen-activated protein kinase/extracellular signal-regulated kinase (MEK) 1/2, MAPKK4/7, and MAPKK3/6 (20). The phosphatidylinositol 3-kinase (PI3-K)/Akt signaling pathway is also important for cell survival and growth and plays a pivotal role in tumorigenesis (21). Elevated expression or excessive activation of PI3-K has been observed in various tumor cells (22–23). Glycogen synthase kinase (GSK)-3β, a downstream target of the PI3-K pathway, causes cyclin D1 degradation in response to mitogenic signals (24–25). PI3-K-dependent phosphorylation of GSK-3β at Ser9 inhibits activation of GSK-3β and thus stabilizes cyclin D1 (25). Therefore, regulation of the PI3-K/Akt/GSK-3βand MKK4 and/or MKK7/JNKs pathways might be a promising strategy for cancer chemoprevention and therapy.

In the present study, we compared the anticancer activity of isoangustone A (IAA; Figure 1A), a novel licorice compound, and glycyrrhizin (Gc; Figure 1B), in SK-MEL-28 cells. In a xenograft model, we found that IAA significantly reduced both the volume and weight of

tumors in nude mice. We further investigated the underlying mechanism of the antitumorigenic effects of IAA.

Materials and Methods

Materials

IAA was obtained as described previously (26). Gc was purchased from Sigma-Aldrich (St. Louis, MO). Dulbecco's Modified Eagle Medium (DMEM) and fetal bovine serum (FBS) were from Gibco BRL (Carlsbad, CA). Antibodies against cyclin D1, cyclin E, CDK4, CDK2, phosphorylated Rb (Ser807/811), Akt (Thr308 and Ser473), GSK3β (Ser9), JNK1/2 (Thr183/Tyr185), p38 (Thr180/Tyr182), MKK4 (Ser257), MKK7 (Ser271/Thr275), and total Rb, Akt, GSK3β, JNK1/2, p38, MKK4, and MKK7 were purchased from Cell Signaling Technology (Beverly, MA). Phosphorylated (Thr202/Tyr204) and total ERK1/2 antibodies were from Santa Cruz Biotechnology (Santa Cruz, CA). Anti-β-actin was from Sigma-Aldrich. CNBr-Sepharose 4B and [γ-^{32}P] ATP were from GE Healthcare (Piscataway, NJ).

Cell culture

SK-MEL-28 and SK-MEL-5 cells were from the American Type Culture Collection (Rockville, MD), and SK-MEL-2 and WM-266–4 cells were from Korean Cell Line Bank at Seoul National University in Seoul, Korea. Human melanoma cells were cultured in monolayers in 10% FBS in DMEM containing 1000 units of penicillin and 1 mg/mL streptomycin at 37°C under 5% CO_2.

Anchorage-independent cell growth assay

The effects of IAA and Gc on anchorage-independent growth were investigated in SK-MEL-28 cells. Cells (8×10^3/mL) were incubated in with or without IAA or Gc (0–20 μM) in 1 mL 0.33% basal medium eagle agar containing 10% FBS, or in 3.5 mL 0.5% basal medium eagle agar containing 10% FBS. The cultures were maintained at 37°C in a 5% CO_2 incubator for 10 days, and cell colonies were counted under a microscope using the Image-Pro Plus software program (Media Cybernetics, Silver Spring, MD).

Cell proliferation assay

Cells were cultured overnight in 96-well plates (3000 cells/well) in 10% FBS/DMEM, and then treated with IAA or Gc at the indicated concentration for 24, 48, or 72 h and 20 μL MTT or MTS reagent were added to each well. For the MTT assay, the media were removed and 200 μL of DMSO were added to each well and absorbance was read at 570 nm. The reduction in MTS was measured 1 h later by spectrophotometry at 492 nm and 690 nm as background (Multiskan MS, Labsystems). Three independent experiments were performed.

Cell cycle analysis

SK-MEL-28 cells were seeded in 60-mm dishes (1.5×10^5 cells/dish) and cultured for 24 h in 10% FBS/DMEM. The cells were treated with IAA or Gc at various concentrations (0–20 μM) and trypsinized 48 h later, washed with ice-cold Dulbecco's phosphate-buffered saline (DPBS) and fixed in ice-cold 70% ethanol at −20°C overnight. Then the cells were washed twice with 20 μg/mL RNase A and 200 μg/mL propidium iodine in DPBS at room temperature (RT) for 30 min in the dark. The cell cycle phase was determined by FACSCalibur (BD Biosciences). Data were gathered using ModFit LT (Verity Software House, Inc., Topsham, ME).

Western blot analysis

SK-MEL-28 cells were cultured for 24 h in 10% FBS/DMEM and then IAA or Gc was added for 24 or 48 h. Then the cells were scraped, treated with lysis buffer (10 mM Tris, pH 7.5, 150 mM NaCl, 5 mM EDTA, 1% Triton X-100, 1 mM dithiothreitol [DTT], 0.1 mM phenylmethylsulfonyl fluoride [PMSF], 10% glycerol, and 1X protease inhibitor cocktail) for 30 min on ice, and centrifuged at 12,000 × *g* for 10 min. For determination of protein levels in SK-MEL-28 xenografts, tumors from each mouse were lysed with T-PER buffer (Pierce). The concentration of protein in the supernatant fractions was measured using a dye-binding protein assay kit, as described by the manufacturer (Bio-Rad Laboratories, Hercules, CA). Lysate aliquots (40 μg protein) were subjected to 10 or 12% SDS-polyacrylamide gel electrophoresis (PAGE) and then transferred to a polyvinylidene fluoride membrane (Millipore Corporation, Bedford, MA). After transfer, the membrane was blocked in 5% fat-free milk for 1 h at RT and incubated with a specific primary antibody at 4°C overnight. After incubation with a horseradish peroxidase-conjugated secondary antibody, protein bands were detected using an enhanced chemiluminescence detection kit (GE Healthcare).

PI3-K assay

An active PI3-K protein (100 ng) was incubated with IAA or LY294002 for 10 min at 30°C. The mixture was incubated with 20 μL of phosphatidylinositol (0.5 mg/mL; Avanti Polar Lipids, Alabaster, AC) for 5 min at RT and then incubated in reaction buffer (100 mM N-2-hydroxyethylpiperazine-N′-2-ethanesulfonic acid, pH 7.6, 50 mM $MgCl_2$, 250 μM ATP containing 10 μCi [γ-^{32}P] ATP) for an additional 10 min at 30°C. The reaction was stopped by adding 15 μL HCl (4 N) and 130 μL chloroform:methanol (1:1). After vortexing, 30 μL of the lower chloroform phase was spotted onto a 1% potassium oxalate-coated silica gel plate, which was previously activated for 1 h at 110°C. The resulting ^{32}P-labeled phosphatidylinositol-3-phosphate was separated by thin-layer chromatography, and the radiolabeled spots were visualized by autoradiography. Relative kinase activity was quantified using Image J.

MKK4 and MKK7 kinase assays

The *in vitro* MKK4 and MKK7 kinase assays were performed following the instructions provided by Upstate Biotechnology (Lake Placid, NY). Briefly, 40 ng active MKK4 or MKK7 recombinant proteins were reacted with IAA (0, 10, or 20 μM) at 30°C for 10 min. For each reaction, 5 μL of 5X kinase buffer (250 mM Tris-HCl, pH 7.5, 0.5 mM EGTA, and 0.5% 2-mercaptoethanol), 5 μL ATP (500 μM), and 2.25 μg inactive JNK1 were added. The mixtures were incubated at 30°C for 15 min. A 5 μL aliquot was removed from the reaction mixture containing 10 μL ATF-2 substrate peptide (2 mg/mL), 5 μL of the 5X kinase buffer, and 5 μL [^{32}P]-ATP (0.16 μCi/μL) solution, and incubated at 30°C for 15 min. Next, 20 μL aliquots were transferred to p81 filter paper and washed 3 times with 1% phosphoric acid for 5 min per wash and once with acetone for 5 min. Radioactive incorporation was determined using a scintillation counter (LS6500; Beckman Coulter). Each experiment was performed 3 times.

Pull-down assays

Recombinant PI3-K (100 ng), MKK4 (200 ng), MKK7 (200 ng) or tumor lysates (500 μg) was incubated with IAA-conjugated Sepharose 4B (or Sepharose 4B as a negative control) beads (100 μL, 50% slurry) in an immunoprecipitation reaction buffer (50 mM Tris-HCl, pH 7.5, 5 mM EDTA, 150 mM NaCl, 1 mM DTT, 0.01% Nonidet P-40, and 0.02 mM phenylmethysulfonyl fluoride) containing 2 μg/mL bovine serum albumin and a 1X protease inhibitor mixture at 4°C overnight with gentle rocking. The beads were washed 5 times with

immunoprecipitation reaction buffer and the protein-bound beads were analyzed by immunoblotting.

ATP and IAA competition assay

Briefly, 100 ng active PI3-K or 200 ng active MKK4 and MKK7 were incubated overnight at 4°C with 0, 10 or 100 μM ATP. Next, 100 μL IAA-Sepharose 4B or 100 μL Sepharose 4B beads were added and incubated overnight at 4°C. Then the samples were washed and the proteins were detected by Western blotting.

Xenograft model

SK-MEL-28 cells (5×10^6 cells/mouse) with 50% Matrigel (BD Bioscience) were injected into male *Balb/c nu/nu* mice and then randomly divided into 3 groups. Based on a previous study (27), vehicle or 2 or 10 mg/kg body weight of IAA were administered by intraperitoneal (i.p) injection daily. Overall body weight was recorded every week and tumor volumes were measured with calipers and calculated using the formula: [π/6 (length) ×(width) ×(height)] until the end of the experiment (5 weeks).

Molecular modeling

Insight II (Accelrys Inc., San Diego, CA) was used for the docking study and structure analysis with the crystal coordinates of PI3-K, MKK4, or MKK7 in complex with ATP or IAA (accession codes 1E8X or 1E90) and are available in the Protein Data Bank (28).

Statistical analysis

When applicable, data are expressed as means ± standard deviation (S.D.). The Student's *t*-test was used for single statistical comparisons. A probability value of $p < 0.05$ was used as the criterion for statistical significance.

Results

IAA is more effective than Gc in attenuating growth of human melanoma cells

To study the effect of IAA on cancer cell growth, we used several human melanoma cell lines, including SK-MEL-2, 5, 28, and WM-266–4. IAA significantly suppressed the growth of all melanoma cells tested (Fig. 1A). We next examined the effect of IAA or Gc on anchorage-independent growth of SK-MEL-28 cells and IAA significantly suppressed growth in a dose-dependent manner (Fig. 1B, a–c). Treatment with 20 μM IAA inhibited the growth of SK-MEL-28 cells up to 67% compared to untreated control cells (Fig. 1B, c). However, Gc had no effect on anchorage-independent growth at concentrations up to 20 μM, (Fig. 1B, d–f).

IAA suppresses proliferation and induces G1 phase cell cycle arrest in SK-MEL-28 cells

Next, we examined the effect of IAA or Gc on proliferation of SK-MEL-28 cells. Compared to Gc, IAA more effectively inhibited proliferation in a dose- and time-dependent manner (Fig. 2A, B). Based on the growth response of SK-MEL-28 cells to IAA, we next examined its effect on cell cycle progression and results revealed that IAA caused cell cycle arrest at G1 phase (Fig. 2C), but treatment with Gc had no effect on cell cycle (Fig. 2D). Because treatment with IAA did not affect the number of cells in sub-G1 (data not shown), IAA-induced growth inhibition was not attributable to apoptosis.

IAA decreases the abundance of G1 phase-related proteins mediated through the Akt/GSK3β and MKK4/MKK7/JNKs signaling pathways

To determine the mechanism responsible for IAA-induced G1 phase cell cycle arrest, we evaluated the expression levels of the various cyclins and CDKs involved in the G1/S phase progression. IAA inhibited the expression of cyclin D1 and cyclin E in SK-MEL-28 cells, whereas Gc had no effect (data not shown). Because phosphorylation of Rb is crucial for S phase transition and is the most recognized substrate of cyclin D-dependent kinases, we determined the effect of IAA or Gc on Rb phosphorylation at Ser807/Ser811, the known sites of Rb phosphorylated by CDK4 (Fig. 3A). IAA substantially suppressed phosphorylation of Rb in a dose-dependent manner in SK-MEL-28 cells. Because the degradation of cyclin D1 is regulated by the PI3-K/Akt/GSK3β signaling cascade (24–25), we examined the effect of IAA on the phosphorylation of Akt and GSK3β. Results showed that IAA inhibited the phosphorylation of Akt (Ser473, Thr308) and GSK3β (Ser9; Fig. 3B). In addition, IAA suppressed the phosphorylation of JNK1/2, but had no effect on ERK1/2 or p38 (Fig. 3C). Next, we examined the effect of IAA on the phosphorylation of MKK4 and MKK7, the upstream kinases of JNK1/2. IAA had no effect on MKK4 or MKK7 phosphorylation (Fig. 3D). These results suggested that an upstream Akt kinase, PI3-K, MKK4 or MKK7 might be potential targets of IAA.

IAA suppresses PI3-K, MKK4, and MKK7 kinase activities by directly binding in an ATP-competitive manner

To investigate whether PI3-K, MKK4, or MKK7 is a molecular target of IAA, we determined the effect of IAA on the *in vitro* kinase activities of these proteins. Treatment with IAA markedly suppressed PI3-K kinase activity in a dose-dependent manner (Fig. 4A). LY294002, a well-known commercially available inhibitor of PI3-K, was used as a positive control. We also found that IAA strongly suppressed MKK4 activity (Fig. 4B) and attenuated MKK7 activity (Fig. 4C) in a dose-dependent fashion. These data indicate that PI3-K, MKK4, and MKK7 are important molecular targets of IAA in the suppression of SK-MEL-28 cell proliferation. Next, we determined whether IAA directly interacts with PI3-K, MKK4, or MKK7 to inhibit their respective kinase activity. Pull-down assay results indicated that PI3-K, MKK4, or MKK7 precipitated with IAA-conjugated Sepharose 4B beads, but not with Sepharose 4B beads only (Fig. 4A–C). These results demonstrated that IAA directly binds to PI3-K, MKK4, or MKK7. ATP treatment blocked the binding ability of IAA with each of these kinases in a dose-dependent manner, suggesting that IAA competes with ATP to bind to each kinase (Fig. 4A–C). These results suggest that inhibition of PI3-K, MKK4, and MKK7 activities by IAA occurs through direct binding of IAA in an ATP-competitive manner.

IAA suppresses xenograft growth of SK-MEL-28 cells

Because IAA effectively suppressed the proliferation of SK-MEL-28 cells, we examined the effects of IAA in an *in vivo* xenograft mouse model. The average volume of tumors in vehicle-injected mice reached 1312 mm^3 at 5 weeks post-injection. However, at this time, the average tumor volume was only 814 or 541 mm^3 inmice treated with 2 or 10 mg/kg IAA, respectively (Fig. 5A). At the end of the study, tumors from each group were removed and weighed. Treatment with IAA (2 or 10 mg/kg) significantly suppressed tumor weight compared to the control group (Fig. S1). IAA treatment did not cause any loss in overall body weight, indicating that the dosages used were not toxic to the animals (Fig. 5B). Furthermore, IAA markedly inhibited the expression of proliferating cell nuclear antigen (PCNA), indicating that IAA could reduce proliferation of SK-MEL-28 cells and tumor growth *in vivo* (Fig. 5C). Tumor lysates from mice treated with 2 or 10 mg/kg of IAA showed decreased phosphorylation levels of Akt (Fig. 5C). Pull-down assays provided

evidence that IAA could bind to the PI3-K, MKK4 and MKK7 in SK-MEL-28 xenograft tumors (Fig. 5D). Collectively, these results suggest that IAA could serve as an effective anticancer agent with the potential to inhibit or delay the tumorigenicity of SK-MEL-28 cells in an *in vivo* system.

Discussion

Licorice is extensively cultivated in China, Korea, Japan, India, and Spain. Licorice root is one of the oldest and most frequently used botanicals and is prescribed as treatment in oriental herbal medicine. Gc is considered the main active compound of licorice (29–32) and is converted by human intestinal bacteria into glycyrrhetic acid (GA) (4). Previous studies showed that both Gc and GA induce apoptosis and inhibit proliferation of melanoma cells (33–34). Gc also has anti-metastatic effects on melanoma *in vitro* and *in vivo* (7). However, effective concentrations of Gc are relatively high, and long-term or large quantities of Gc consumption result in side effects such as mineralocorticoid excess, hypertension, and hypokalemia (8, 35). In addition to triterpenoids, about 300 polyphenols are in dried licorice root (35). In the current study, we determined that a novel polyphenol licorice compound, IAA, suppressed both anchorage-independent and anchorage-dependent growth of SK-MEL-28 cells better than Gc. IAA also inhibited xenograft growth of SK-MEL-28 cells in mice.

Unregulated cell growth is a critical characteristic of cancer cells and a primary requirement for cancer progression (36). Abundant evidence indicates that cell cycle deregulation plays a crucial role in several types of human cancer (17, 37). Cyclin D1 regulates CDK4 and CDK6 holoenzyme complexes, which phosphorylate and deactivate the tumor suppressor protein Rb. The CDK4 or 6/cyclin D and CDK2/cyclin E complexes regulate progression from the G1 to the S phase of the cell cycle (25). We determined that treatment with IAA, but not Gc, induced G1 phase arrest in SK-MEL-28 cells. IAA also inhibited G1 phase-related proteins, including cyclin D1 and cyclin E, whereas Gc had no effect. Our data demonstrate that IAA suppresses proliferation by inducing G1 phase cell cycle arrest.

PI3-K and MAPKs pathways are involved in melanoma development by relaying extracellular signals to regulate diverse cellular processes, including proliferation, cell survival, invasion, and angiogenesis (38–39). PI3-K/Akt-dependent pathways regulate the expression of cyclin D1. Akt phosphorylates GSK-3β at Ser9, thereby decreasing GSK-3β activity and stabilizing cyclin D1 expression (25). Therefore, we determined whether IAA affected the PI3-K/Akt/GSK-3β pathway and our data showed that IAA suppresses phosphorylation of both Akt and GSK-3β.

We hypothesized that the molecular target of IAA for arresting G1 phase might be upstream kinases of Akt or JNK1/2. We found that IAA can effectively and directly bind to and inhibit PI3-K, MKK4 and MKK7 activities, resulting in the attenuation of Akt/GSK-3β and JNK1/2 signaling. Furthermore, IAA competed with ATP for binding, which could explain the reduced activity of these kinases. Collectively, these results suggest that inhibition of cyclin D1 expression by IAA is primarily the result of the direct suppression of PI3-K, MKK4 and MKK7 activities.

In light of our experimental finding showing that IAA inhibits the activities of PI3-K, MKK4 and MKK7, we performed a molecular docking study to investigate the binding mode of IAA to these proteins. We allowed both the ligand molecule and the amino acids constituting the binding pocket to be flexible. Figure 6A (upper panel) shows the docking conformation of IAA in the ATP-binding pocket of PI3-K. The diagram of the PI3-K interaction with IAA is shown in Figure 6A (upper panel). IAA forms hydrogen bonds with

the backbone carbonyl oxygen of Ala885 and the side chain carboxylate oxygen of Asp964. It is further stabilized by favorable interactions with polar amino acids Thr887, Thr886, and Asn951, a positively charged residue (Lys833), and a negatively charged residue (Asp836). Lys833 interacts with the alpha phosphate of ATP, and this residue is conserved in all PI3-Ks. Our docking study also showed that the interaction of IAA with Lys833 helps stabilize the protein-ligand complex. The upper and lower regions, as well as the hydrocarbon chains of the ligand molecules, are stabilized by hydrophobic interactions with several hydrophobic amino acids, including Trp812, Ile881, Met953, Ile831, Ile963, Ile879, Tyr867, Phe965, Leu838, and Leu845. The hydrophobic pocket constituting these amino acids is shown in Figure 6A (upper panel). Our modeling study showed that IAA binds to the ATP-binding pocket of PI3-K.

Figure 6A (middle panel) shows IAA docked to the ATP-binding pocket of MKK4. In the MKK4 protein, the ATP-binding pocket is located at the interface of the N- and C-terminal lobes of the enzyme. The drug molecule forms three hydrogen bonds with the enzyme. Two of the three are within the hinge region of MKK4 and involve the -CO backbone of Glu179 and the -NH backbone of Met181. The third hydrogen bond is with the side chain carboxylate oxygen of Asp186. As shown, Lys260 from the activation loop strongly interacts with one of the hydroxyl groups of IAA. Similarly, the polar amino acids Thr183 and Ser184 favorably interact with this compound. Similar to MKK7 and PI3-K, the upper and lower regions of IAA are surrounded by several hydrophobic residues, adding stability to the protein-ligand complex. These results demonstrate that IAA can bind to MKK4 at the ATP-binding pocket.

Figure 6A (lower panel) shows the docking model of IAA bound to the ATP-binding pocket of MKK7. The ATP-binding pocket is located at the interface of the N- and C-terminal lobes of MKK7. IAA forms two hydrogen bonds with the hinge region of MKK7, involving the -CO backbone of Glu240 and the -NH backbone of Met 242, and a third hydrogen bond with the -CO backbone of Met169. The side chain functional groups of Lys248 and Glu168 interact favorably with the hydroxyl groups of IAA. The upper and lower regions of the ligand molecule are surrounded by a hydrophobic pocket constituting several hydrophobic residues. Our modeling results showed that IAA can bind to MKK7 at the ATP-binding pocket. Overall, these results demonstrate that IAA can bind to the ATP-binding pocket of PI3-K, MKK4, and MKK7, which is consistent with the experimental observations.

A recently adopted strategy in anticancer therapeutics is the development of agents that target a variety of kinases. Two multi-targeting kinase inhibitors, sunitinib and sorafenib, have been shown to be effective in clinical testing (40–41). The rationale behind this strategy is that these agents will be more effective by suppressing multiple oncogenic pathways than the highly selective kinase inhibitors administered as single agents (42). In our study, we found that IAA was capable of targeting PI3K, MKK4 and MKK7. IAA markedly inhibits proliferation of human melanoma cells and showed no toxicity in Melan-A normal melanocytes, up to 20 μM (Fig. S1). *In vivo* xenograft results also showed that IAA effectively suppresses SK-MEL-28 tumor growth without loss of weight in mice (Fig. 5B). All of these results suggested that the potency of IAA against melanoma cells could be at least partially attributable to the fact that IAA reduces several proliferation signals rather than only one.

Overall, in the present study, IAA suppressed anchorage-independent and anchorage-dependent proliferation of human melanoma cells by substantially blocking cell cycle progression at the G1 phase. IAA inhibited the expression of G1 phase-related proteins, including cyclin D1 and cyclin E, and also attenuated phosphorylation of Rb. IAA bound to PI3-K, MKK4 and MKK7. The licorice compound suppressed their respective kinase

activity, thereby blocking the Akt/GSK-3β and JNK1/2 signaling pathways, and subsequently reduced cyclin D1 expression. A simplified depiction of our proposed mechanism for the anti-proliferative effects of IAA is shown in Figure 6B. Collectively, these results suggest that PI3-K, MKK4 and MKK7 are the primary molecular targets of IAA in the suppression of SK-MEL-28 melanoma cell proliferation. This insight into the biological actions of IAA might provide a molecular basis for the development of new anticancer agents.

Supplementary Material

Refer to Web version on PubMed Central for supplementary material.

Acknowledgments

Grant support: National Leap Research Program (No. 2010-0029233); Global Frontier Project grant (NRF-M1AXA002-2012M3A6A4054949) through the National Research Foundation of Korea funded by the Ministry of Education, Science and Technology of Korea; 2012 High Value Added Food industry Professional Human Resources Development Project, Ministry of Agriculture, Food and Runal Affairs, Republic of Korea (H. J. Lee, K. W. Lee); The Hormel Foundation and National Institutes of Health grants CA172457, CA1666011, CA077646, CA088646 and ES016548 (Z. Dong)

References

1. Dhiman RK, Chawla YK. Herbal medicines for liver diseases. Dig Dis Sci. 2005; 50:1807–12. [PubMed: 16187178]
2. Fuhrman B, Volkova N, Kaplan M, Presser D, Attias J, Hayek T, et al. Antiatherosclerotic effects of licorice extract supplementation on hypercholesterolemic patients: increased resistance of LDL to atherogenic modifications, reduced plasma lipid levels, and decreased systolic blood pressure. Nutrition. 2002; 18:268–73. [PubMed: 11882402]
3. Fukai T, Marumo A, Kaitou K, Kanda T, Terada S, Nomura T. Anti-Helicobacter pylori flavonoids from licorice extract. Life Sci. 2002; 71:1449–63. [PubMed: 12127165]
4. Wang ZY, Nixon DW. Licorice and cancer. Nutr Cancer. 2001; 39:1–11. [PubMed: 11588889]
5. Aydemir EA, Oz ES, Gokturk RS, Ozkan G, Fiskin K. Glycyrrhiza flavescens subsp. antalyensis exerts antiproliferative effects on melanoma cells via altering TNF-alpha and IFN-alpha levels. Food Chem Toxicol. 2011; 49:820–8. [PubMed: 21145935]
6. Kobayashi M, Fujita K, Katakura T, Utsunomiya T, Pollard RB, Suzuki F. Inhibitory effect of glycyrrhizin on experimental pulmonary metastasis in mice inoculated with B16 melanoma. Anticancer Res. 2002; 22:4053–8. [PubMed: 12553032]
7. Rossi T, Benassi L, Magnoni C, Ruberto AI, Coppi A, Baggio G. Effects of glycyrrhizin on UVB-irradiated melanoma cells. In Vivo. 2005; 19:319–22. [PubMed: 15796192]
8. Shintani S, Murase H, Tsukagoshi H, Shiigai T. Glycyrrhizin (licorice)-induced hypokalemic myopathy. Report of 2 cases and review of the literature. Eur Neurol. 1992; 32:44–51. [PubMed: 1563455]
9. Stormer FC, Reistad R, Alexander J. Glycyrrhizic acid in liquorice--evaluation of health hazard. Food Chem Toxicol. 1993; 31:303–12. [PubMed: 8386690]
10. Malumbres M, Barbacid M. Cell cycle, CDKs and cancer: a changing paradigm. Nat Rev Cancer. 2009; 9:153–66. [PubMed: 19238148]
11. Vermeulen K, Van Bockstaele DR, Berneman ZN. The cell cycle: a review of regulation, deregulation and therapeutic targets in cancer. Cell Prolif. 2003; 36:131–49. [PubMed: 12814430]
12. Sherr CJ. D-type cyclins. Trends Biochem Sci. 1995; 20:187–90. [PubMed: 7610482]
13. Sherr CJ. Cancer cell cycles. Science. 1996; 274:1672–7. [PubMed: 8939849]
14. Barbieri F, Lorenzi P, Ragni N, Schettini G, Bruzzo C, Pedulla F, et al. Overexpression of cyclin D1 is associated with poor survival in epithelial ovarian cancer. Oncology. 2004; 66:310–5. [PubMed: 15218299]

15. Fu M, Wang C, Li Z, Sakamaki T, Pestell RG. Minireview: Cyclin D1: normal and abnormal functions. Endocrinology. 2004; 145:5439–47. [PubMed: 15331580]
16. Utsunomiya T, Doki Y, Takemoto H, Shiozaki H, Yano M, Sekimoto M, et al. Correlation of beta-catenin and cyclin D1 expression in colon cancers. Oncology. 2001; 61:226–33. [PubMed: 11574779]
17. Musgrove EA, Caldon CE, Barraclough J, Stone A, Sutherland RL. Cyclin D as a therapeutic target in cancer. Nat Rev Cancer. 2011; 11:558–72. [PubMed: 21734724]
18. Bastian BC, Kashani-Sabet M, Hamm H, Godfrey T, Moore DH 2nd, Brocker EB, et al. Gene amplifications characterize acral melanoma and permit the detection of occult tumor cells in the surrounding skin. Cancer Res. 2000; 60:1968–73. [PubMed: 10766187]
19. Curtin JA, Fridlyand J, Kageshita T, Patel HN, Busam KJ, Kutzner H, et al. Distinct sets of genetic alterations in melanoma. N Engl J Med. 2005; 353:2135–47. [PubMed: 16291983]
20. Chang L, Karin M. Mammalian MAP kinase signalling cascades. Nature. 2001; 410:37–40. [PubMed: 11242034]
21. Willems L, Tamburini J, Chapuis N, Lacombe C, Mayeux P, Bouscary D. PI3K and mTOR signaling pathways in cancer: new data on targeted therapies. Curr Oncol Rep. 2012; 14:129–38. [PubMed: 22350330]
22. Steelman LS, Stadelman KM, Chappell WH, Horn S, Basecke J, Cervello M, et al. Akt as a therapeutic target in cancer. Expert Opin Ther Targets. 2008; 12:1139–65. [PubMed: 18694380]
23. Yuan TL, Cantley LC. PI3K pathway alterations in cancer: variations on a theme. Oncogene. 2008; 27:5497–510. [PubMed: 18794884]
24. Liang J, Slingerland JM. Multiple roles of the PI3K/PKB (Akt) pathway in cell cycle progression. Cell Cycle. 2003; 2:339–45. [PubMed: 12851486]
25. Takahashi-Yanaga F, Sasaguri T. GSK-3beta regulates cyclin D1 expression: a new target for chemotherapy. Cell Signal. 2008; 20:581–9. [PubMed: 18023328]
26. Lee YS, Kim SH, Kim JK, Shin HK, Kang YH, Park JH, et al. Rapid identification and preparative isolation of antioxidant components in licorice. J Sep Sci. 2010; 33:664–71. [PubMed: 20112307]
27. Lee E, Son JE, Byun S, Lee SJ, Kim YA, Liu K, et al. CDK2 and mTOR are direct molecular targets of isoangustone A in the suppression of human prostate cancer cell growth. Toxicol Appl Pharmacol. 2013; 272:12–20. [PubMed: 23707764]
28. Bernstein FC, Koetzle TF, Williams GJ, Meyer EF Jr, Brice MD, Rodgers JR, et al. The Protein Data Bank: a computer-based archival file for macromolecular structures. J Mol Biol. 1977; 112:535–42. [PubMed: 875032]
29. Akimoto M, Kimura M, Sawano A, Iwasaki H, Nakajima Y, Matano S, et al. Prevention of cancer chemotherapeutic agent-induced toxicity in postoperative breast cancer patients with glycyrrhizin (SNMC). Gan No Rinsho. 1986; 32:869–72. [PubMed: 3091882]
30. Arase Y, Ikeda K, Murashima N, Chayama K, Tsubota A, Koida I, et al. The long term efficacy of glycyrrhizin in chronic hepatitis C patients. Cancer. 1997; 79:1494–500. [PubMed: 9118029]
31. Nomura T, Fukai T. Phenolic constituents of licorice (Glycyrrhiza species). Fortschr Chem Org Naturst. 1998; 73:1–158. [PubMed: 9545874]
32. Yasukawa K, Takido M, Takeuchi M, Nakagawa S. Inhibitory effect of glycyrrhizin and caffeine on two-stage carcinogenesis in mice. Yakugaku Zasshi. 1988; 108:794–6. [PubMed: 3150008]
33. Abe H, Ohya N, Yamamoto KF, Shibuya T, Arichi S, Odashima S. Effects of glycyrrhizin and glycyrrhetinic acid on growth and melanogenesis in cultured B16 melanoma cells. Eur J Cancer Clin Oncol. 1987; 23:1549–55. [PubMed: 3678319]
34. Liu W, Kato M, Akhand AA, Hayakawa A, Takemura M, Yoshida S, et al. The herbal medicine sho-saiko-to inhibits the growth of malignant melanoma cells by upregulating Fas-mediated apoptosis and arresting cell cycle through downregulation of cyclin dependent kinases. Int J Oncol. 1998; 12:1321–6. [PubMed: 9592193]
35. Johns C. Glycyrrhizic acid toxicity caused by consumption of licorice candy cigars. CJEM. 2009; 11:94–6. [PubMed: 19166646]
36. Nguyen-Ba G, Vasseur P. Epigenetic events during the process of cell transformation induced by carcinogens (review). Oncol Rep. 1999; 6:925–32. [PubMed: 10373683]

37. Draetta GF. Mammalian G1 cyclins. Curr Opin Cell Biol. 1994; 6:842–6. [PubMed: 7880531]
38. Davies MA. The role of the PI3K-AKT pathway in melanoma. Cancer J. 2012; 18:142–7. [PubMed: 22453015]
39. Lopez-Bergami P. The role of mitogen- and stress-activated protein kinase pathways in melanoma. Pigment cell & melanoma research. 2011; 24:902–21. [PubMed: 21914141]
40. Raymond E, Hammel P, Dreyer C, Maatescu C, Hentic O, Ruszniewski P, et al. Sunitinib in pancreatic neuroendocrine tumors. Target Oncol. 2012; 7:117–25. [PubMed: 22661319]
41. Sciarra A, Gentile V, Salciccia S, Alfarone A, Di Silverio F. New anti-angiogenic targeted therapy in advanced renal cell carcinoma (RCC): current status and future prospects. Rev Recent Clin Trials. 2008; 3:97–103. [PubMed: 18474019]
42. Petrelli A, Valabrega G. Multitarget drugs: the present and the future of cancer therapy. Expert Opin Pharmacother. 2009; 10:589–600. [PubMed: 19284362]

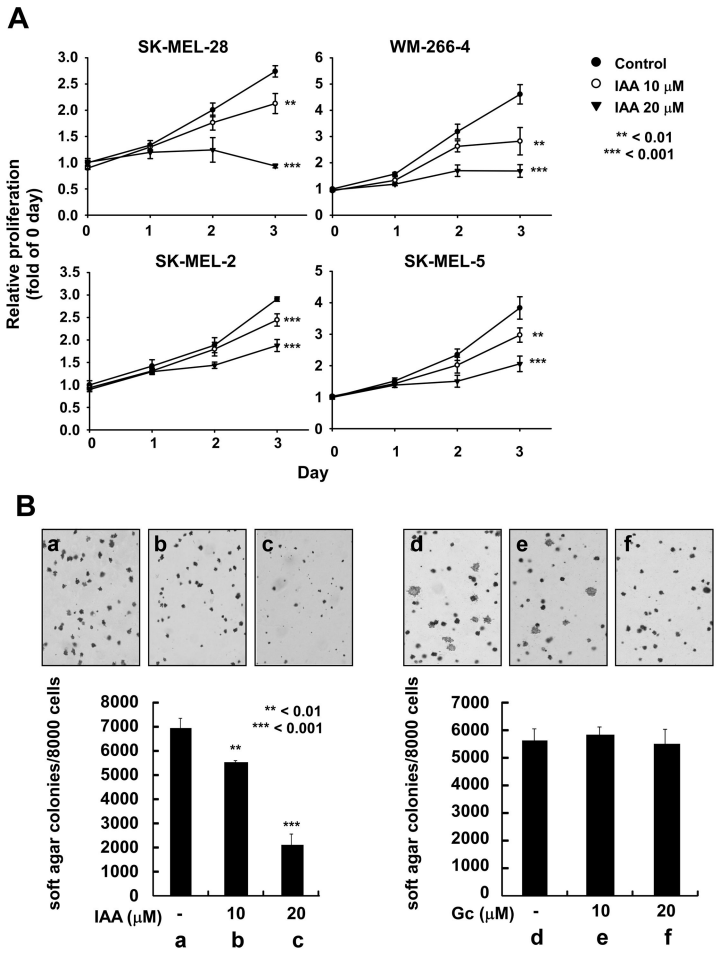

Figure 1.

The effect of IAA and Gc on growth of human melanoma cells. A) IAA suppresses growth of SK-MEL-2, 5, 28, and WM-266–4 human melanoma cells. Proliferation levels were measured by MTT assay. The asterisks indicate significant differences between treated groups and untreated controls (**$p < 0.01$, ***0.001). B) IAA inhibits anchorage-independent growth of SK-MEL-28 cells (a, untreated control; b, 10 μM IAA; c, 20 μM IAA). Gc has no effect on anchorage-independent growth of SK-MEL-28 cells (d, untreated control; e, 10 μM Gc; f, 20 μM Gc). Data are presented as means ± S.D. of the number of colonies determined from 3 independent experiments. The asterisks indicate a significant (**p < 0.01, ***p < 0.001) decrease in the number of colonies after treatment with IAA versus untreated control group.

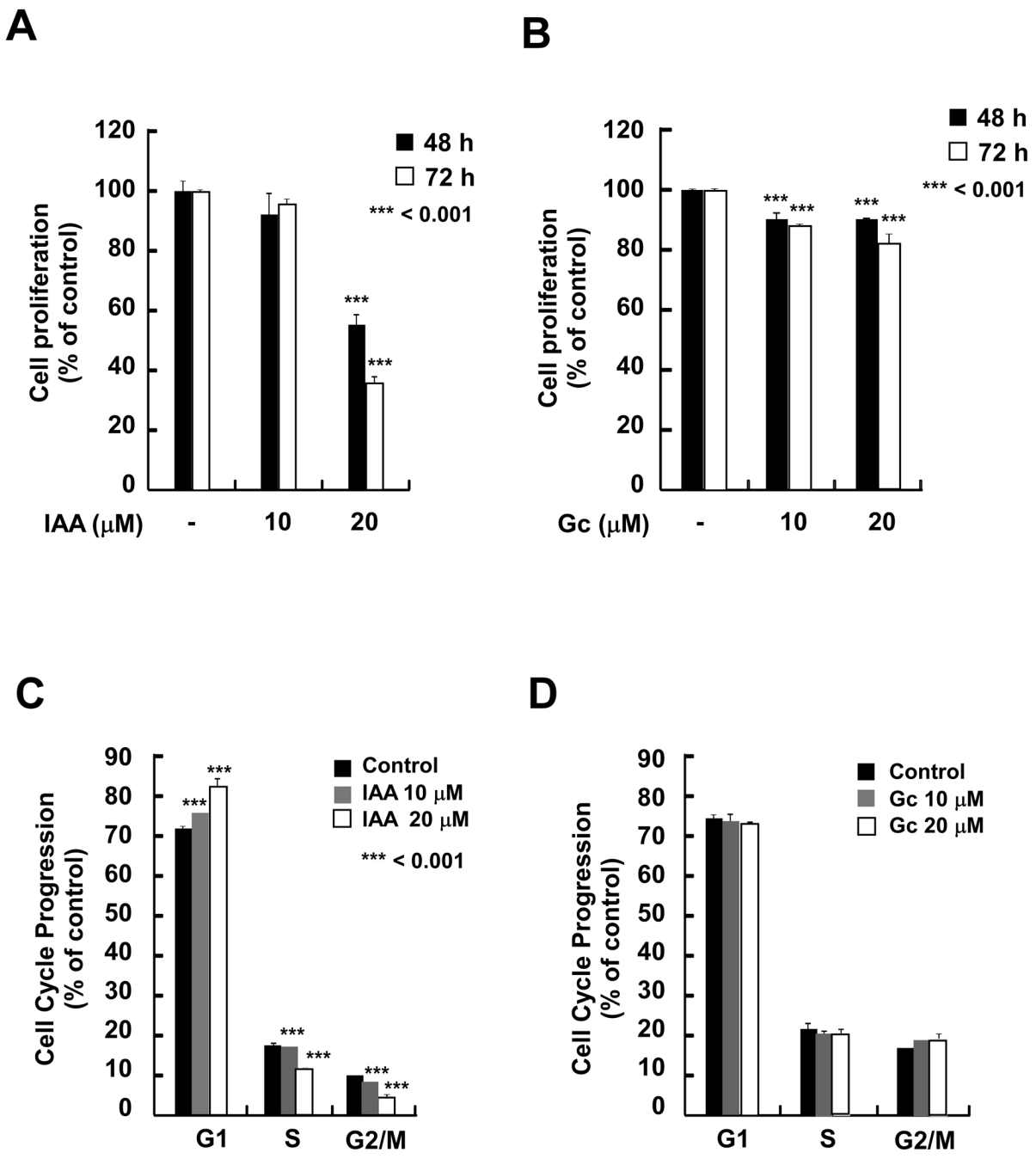

Figure 2.

The effects of IAA and Gc on proliferation and cell cycle distribution. A and B) IAA, not Gc, suppresses anchorage-dependent growth of SK-MEL-28 cells. SK-MEL-28 cells were treated with IAA (A) or Gc (B) (0, 10, or 20 μM) for the indicated times. Proliferation was determined by MTS assay. C and D) IAA, not Gc, causes SK-MEL-28 cell cycle arrest at G1 phase. Cells were treated with IAA (C) or Gc (D) at the indicated concentrations for 48 h. The effects of IAA and Gc on cell cycle distribution are presented as the percent of IAA- or Gc-treated cells at the G1, S, or G2/M phase of cell cycle compared to untreated control cells. Data are shown as means ± S.D. of 3 samples from 3 independent experiments. The

asterisks indicate a significant difference (***$p < 0.001$) in the number of cells after treatment with IAA versus untreated control group.

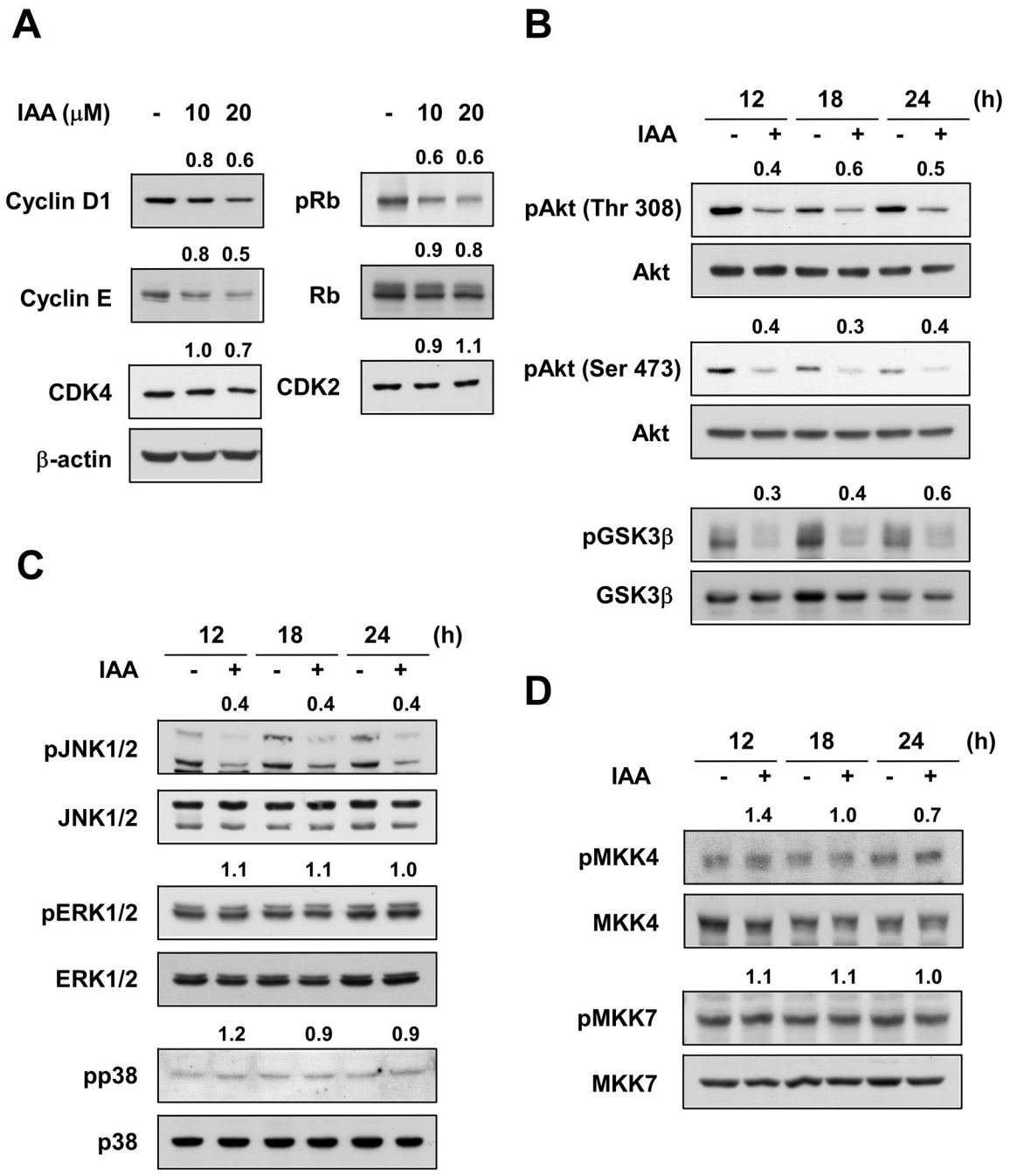

Figure 3.

Effects of IAA on expression of G1 phase regulatory proteins and Akt and MAPK signaling pathways in SK-MEL-28 cells. A) IAA inhibits the expression of cyclin D1 and cyclin E, and Rb phosphorylation in SK-MEL-28 cells. Cells were treated 48 h with IAA at the indicated concentrations. The protein level was determined by Western blot using specific antibodies. Data are representative of 3 independent experiments. Numbers above each band indicate relative density normalized to β-actin (cyclin D1, cyclin E, Rb, CDK4, and CDK2) or total-Rb (p-Rb). B, C, and D) Effect of IAA on phosphorylation of Akt and GSK3β (B), JNK1/2 (C), MKK4 and MKK7 (D) in SK-MEL-28 cells. IAA has no effect on the phosphorylation of ERK1/2 or p38 (C). Cells were treated with IAA (20 μM) and harvested

at the indicated times. The level of phosphorylated and total proteins was determined by Western blot. Data are representative of 3 independent experiments. Numbers above each band show the relative normalized phosphorylation levels versus control at each time point.

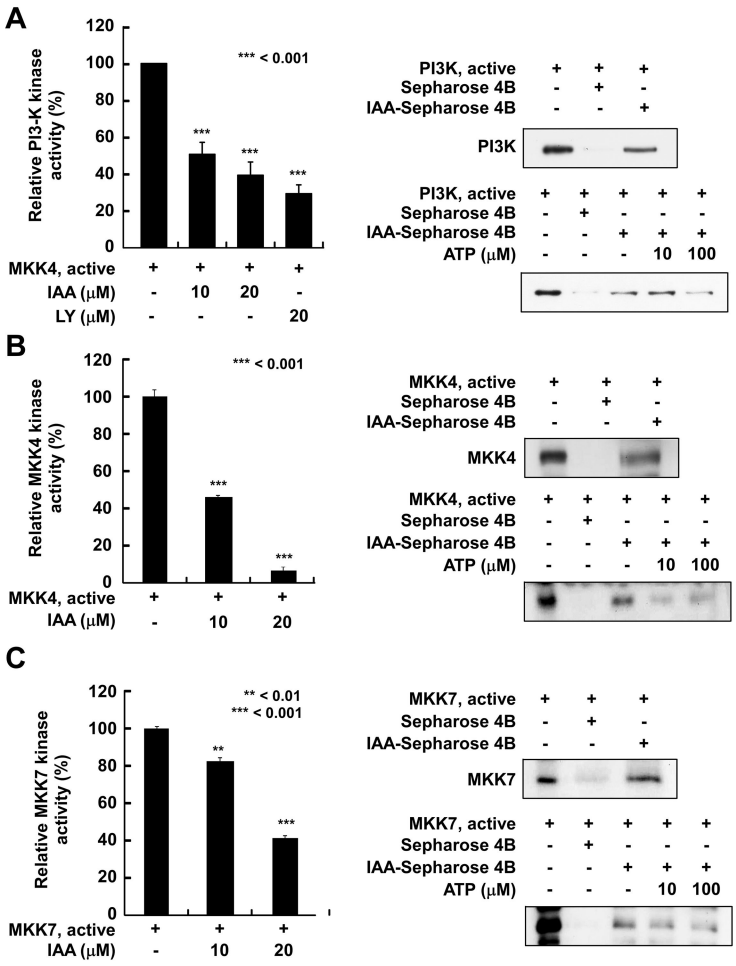

Figure 4.

IAA inhibits PI3-K, MKK4, and MKK7 kinase activities by directly binding in an ATP-competitive manner. A, *left*) IAA suppresses *in vitro* PI3-K activity by directly binding in an ATP-competitive manner. Active PI3-K (100 ng) was incubated with IAA or LY294002 at the indicated concentrations for 10 min at 30°C and then incubated with the phosphatidylinositol substrate and [γ-^{32}P]ATP for an additional 10 min at 30°C. Data are representative of 3 independent experiments. Density of each spot was measured using Image J. B and C, *left*) IAA inhibits MKK4 and MKK7 kinase activities *in vitro*. Kinase activity is expressed as percent inhibition relative to untreated control activity. The average ^{32}P was determined from 3 independent experiments. Data are presented as means ± S.D. The asterisks indicate a significant decrease (**p < 0.01 or ***0.001) in kinase activity after treatment with IAA versus untreated control group. A–C, *upper right*) The binding of IAA to PI3-K, MKK4, and MKK7 was confirmed by immunoblotting using antibodies against PI3-K (p110), MKK4, or MKK7 (lane 1: input control, PI3-K, MKK4, or MKK7 protein standard; lane 2: control). Sepharose 4B beads alone or conjugated to IAA were used to pull down PI3-K, MKK4, or MKK7 (lane 3). A–C, *bottom right*) IAA competes with ATP to bind PI3-K, MKK4, or MKK7. Active PI3-K (100 ng), MKK4, or MKK7 (200 ng) was incubated with ATP at different concentrations (0, 10, or 100 μM) and either 100 μL IAA-Sepharose 4B or 100 μL Sepharose 4B (negative control) in reaction buffer (final volume, 500 μL). The mixtures were incubated at 4°C overnight with shaking. After washing, the proteins were detected by Western blotting (lane 1: input control, PI3-K,

MKK4, or MKK7 protein standard; lane 2: negative control, PI3-K, MKK4, or MKK7 bound to Sepharose 4B; lane 3: positive control, PI3K, MKK4, or MKK7 binding to IAA-Sepharose 4B). Each experiment was performed 3 times and representative blots are shown.

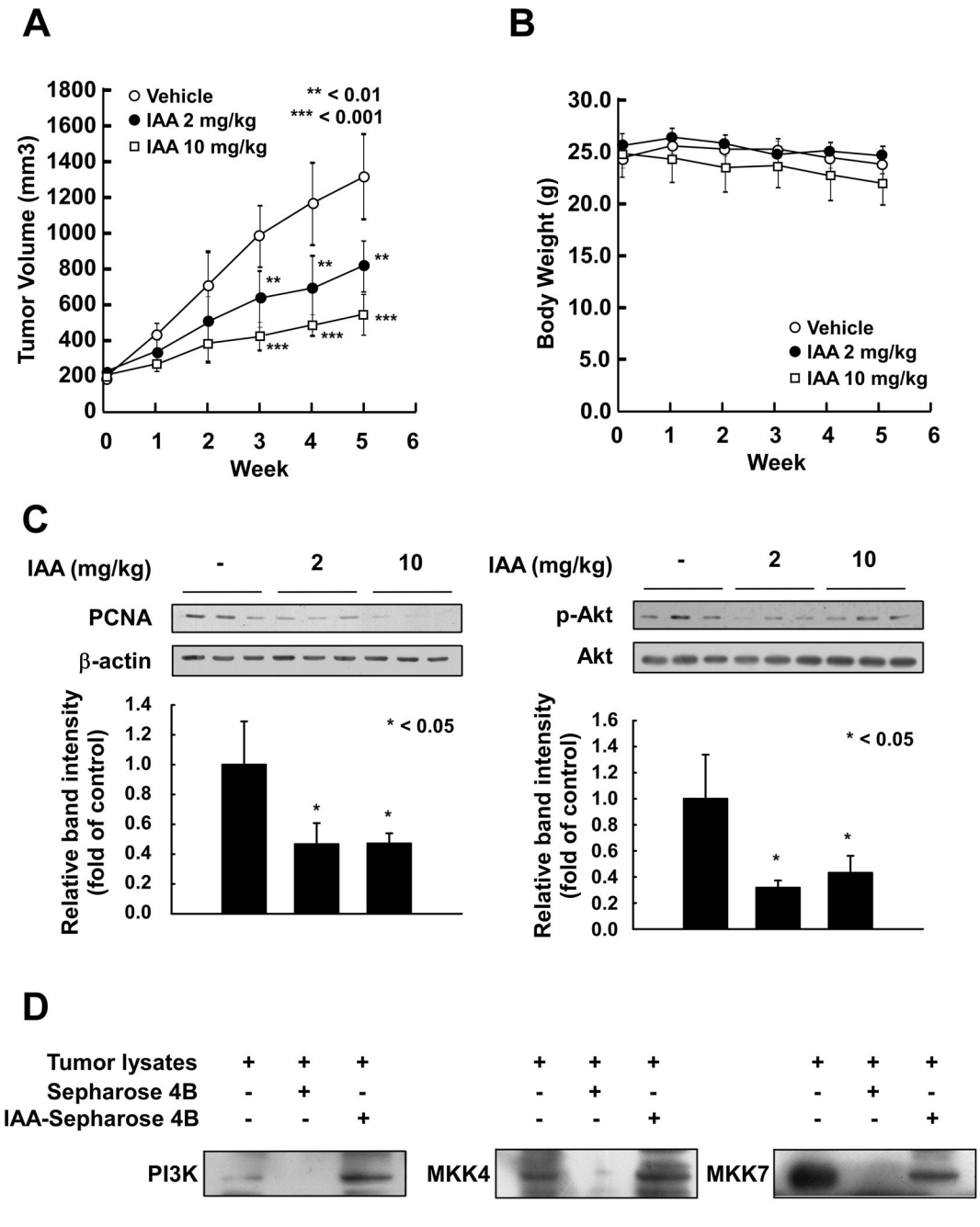

Figure 5.

The effect of IAA on tumor growth in an SK-MEL-28 xenograft model. A) The average tumor volume of control and IAA-treated mice plotted over 35 days after tumor cell injection. The p-values indicate statistical significance of the inhibition of tumor growth by IAA (**p < 0.01, ***p < 0.001). B) Average body weights (measured weekly) of mice treated with IAA concentrations of 2 or 10 mg/kg were not significantly different compared to controls. C) IAA reduced PCNA expression and phosphorylation of Akt (Ser473) in xenograft tumors. Quantified results (Image J) are presented as graphs. The asterisk indicates statistical significance of IAA-treated groups versus control group (* $p < 0.05$). D) IAA binds with PI3-K (*left*), MKK4 (*middle*), and MKK7 (*right*) in SK-MEL-28 xenografts tumors. *Lane 1*, tumor lysates as input; *Lane 2*, Negative control, PI3-K, MKK4, and MKK7

do not bind with Sepharose 4B; *Lane 3*, Positive control, PI3-K, MKK4, and MKK7 bind with IAA–Sepharose 4B *in vivo*.

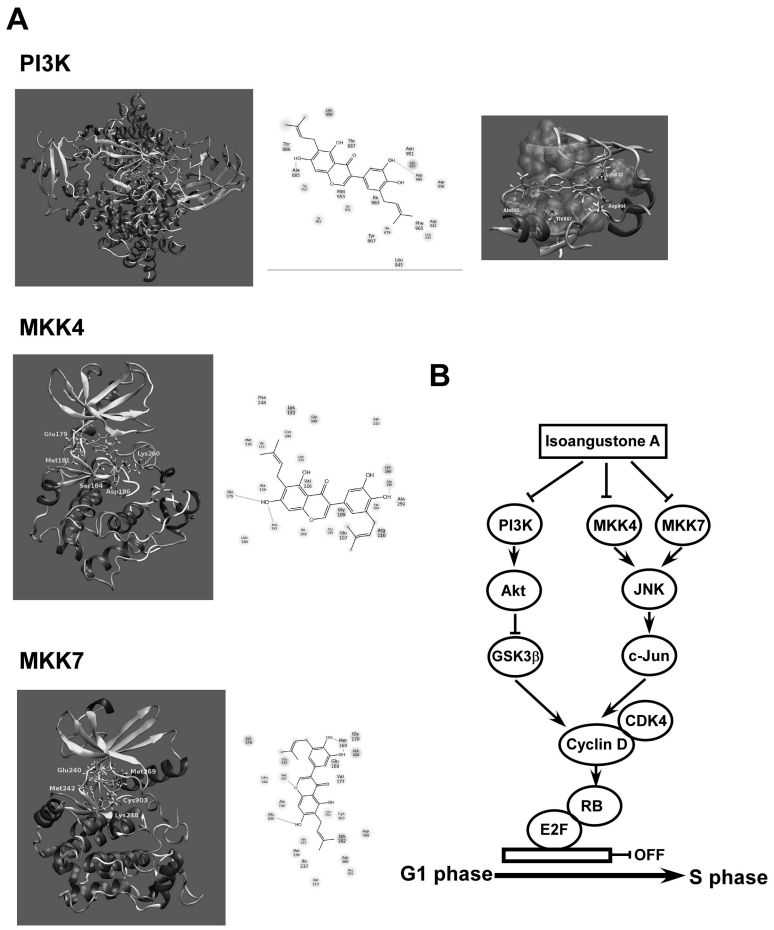

Figure 6.
Modeling of IAA with PI3-K, MKK4, or MKK7. A) The docking conformation of IAA in the ATP-binding pocket of PI3-K, MKK4, and MKK7. B) Hypothetical scheme of the mechanism of the anti-proliferative action of IAA.